POLITECNICO DI TORINO
Repository ISTITUZIONALE

Decentralized Neyman-Pearson Test with Belief Propagation for Peer-to-Peer Collaborative Spectrum Sensing

(Article begins on next page)

29 March 2023

Decentralized Neyman-Pearson Test with Belief Propagation for Peer-to-Peer Collaborative Spectrum Sensing

Federico Penna, *Student Member, IEEE*, and Roberto Garello, *Senior Member, IEEE*

Abstract—In this paper we propose a decentralized approach for cooperative signal detection, based on peer-to-peer collaboration among sensor nodes. The proposed method combines belief propagation, implemented in a distributed fashion through the exchange of local messages to and from neighboring nodes, with a Neyman-Pearson framework, that allows control over the false-alarm rate of each node. At the same time, nodes gradually learn their degree of correlation with neighbors, and clusters of nodes under homogeneous conditions are formed automatically. The performance of the resulting "Neyman-Pearson belief propagation" (NP-BP) algorithm is shown to be nearly equivalent to that of cooperative energy detection applied separately at each cluster. Thanks to its decentralized structure, NP-BP provides improved robustness, flexibility, and scalability compared to traditional, centralized schemes. In addition, its ability to adaptively form clusters makes the algorithm suitable for heterogeneous or time-varying radio environments.

Index Terms—Multi-sensor signal detection, cognitive radio, distributed Neyman-Pearson test, belief propagation, sum-product algorithm, Markov random fields.

I. INTRODUCTION AND RELATED WORKS

DISTRIBUTED signal detection has been extensively investigated over the last decades. Research in this area has been motivated by applications such as multi-sensor surveillance systems [1]–[5] and, more recently, collaborative spectrum sensing in cognitive radio systems [6]–[10]. Problems of distributed detection and estimation are also studied in the literature of sensor networks [11]–[13].

Regardless of the specific application, distributed signal detection problems can be classified as follows.

- According to the problem configuration: if all sensors observe the same event ($\mathcal{H} = 0$ or $\mathcal{H} = 1$), we refer to *homogeneous* or *global* detection problems; if different sensors may observe different, localized events, we refer to *heterogeneous* or *local* detection problems.
- According to the approach: the *Bayesian* approach assumes prior distributions of the two alternative events ($\mathcal{H} = 0$: signal absent, $\mathcal{H} = 1$: signal present) and aims at maximizing an *a posteriori* likelihood function; the *Neyman-Pearson (NP)* approach, on the contrary, uses as test statistic the likelihood of observations, and aims at maximizing the probability of detection given a constraint on the false-alarm rate.
- According to the architecture: distributed systems may be *centralized* (if there is a fusion center which processes the data sent from the other sensors), or *decentralized* (if all sensors behave as peers and work without a central control unit)[1].

In this paper we focus on spectrum sensing applications. With respect to the above classification, the problem of multi-sensor signal detection for spectrum sensing has been traditionally treated as a *homogeneous* detection problem (all sensors are to detect the presence of the same primary signal), addressed from a *NP* perspective (motivated by the fact that cognitive radio systems should meet fixed constraints on the false-alarm and missed-detection rates), assuming the existence of a fusion center (*centralized* architecture).

Attempts to map cooperative spectrum sensing to a fully decentralized architecture, while at the same time considering a heterogeneous problem setting, include [14] and our previous work [15]. These two papers independently proposed the use of a decentralized implementation of the belief propagation (BP) algorithm [21], in which nodes' test statistics are iteratively updated by exchanging peer-to-peer messages. We denote this approach *peer-to-peer collaborative spectrum sensing*, where the term "peer-to-peer" is used to emphasize the absence of hierarchical structures (e.g., fusion centers or predefined clusters): network-wide cooperation is gradually achieved through iterative exchange of local, peer-to-peer messages. Previously, in [22] BP was introduced as a computational tool for spectrum sensing, but still assuming a traditional architecture with a fusion center. On the other hand, examples of decentralized BP over wireless networks had appeared in the literature of cooperative positioning [23], [24] and sensor networks [11].

Both [14] and [15] adopt Bayesian approaches. The main inconvenience with Bayesian detection is that it does not make it possible to precisely select the decision threshold as a function of a target false-alarm rate. Typically, in the Bayesian framework, costs are associated to the events of false alarm and missed detection, and the threshold can be chosen so as to minimize the total expected cost. In this

[1]Note that this terminology is not universal: in the literature the word "distributed" is sometimes used as a synonym of "decentralized". To avoid any ambiguity, in this paper we use "distributed" with a general meaning of "multi-sensor", and we then distinguish between centralized and decentralized architectures.

paper we combine the peer-to-peer collaborative spectrum sensing approach, based on the BP algorithm, with local Neyman-Pearson tests, allowing for a precise control of the false-alarm probability of each node, as needed in cognitive radio applications. Note that a similar problem (applied to sensor networks, and generalized to multivariate observations) is addressed in [13] by another method that, in contrast to the NP approach, aims at minimizing the expected global "false discovery rate" over all network nodes.

Similar to [15], we model the dependency among neighboring nodes through a pairwise Markov random field (MRF). We introduce here a simple algorithm to learn the values of such inter-dependencies based on a certain observation window. This algorithm results in automatic clustering of the groups of nodes that observe similar data. We will show that, after a sufficient learning period, the detection performance of each single node converges to that achieved by the relevant cluster performing centralized cooperative energy detection. At the same time, if the statistical correlation between two neighboring nodes vanishes, the proposed learning procedure ensures that the detection performance of both nodes is restored to the original single-node level within a limited number of time slots.

The paper is organized as follows. In Sec. II we define a mathematical system model, we introduce basic concepts of signal detection, and we present a model for statistical correlations between neighboring nodes. In Sec. III we introduce the BP algorithm and we discuss its application in the considered NP framework. In Sec. IV we analyze the performance of the proposed NP-BP algorithm, thus deriving expressions for the decision threshold and for the detection probability of the algorithm; we then discuss the impact of cycles in the graph. In Sec. V we illustrate the performance of NP-BP by numerical simulations. Conclusions are drawn in Sec. VI.

II. MATHEMATICAL FORMULATION

A. System Model

We consider a cognitive network composed of K "secondary" users, coexisting with a "primary" network. The channel occupation for a certain secondary node k at time t is denoted by $\mathcal{H}_k^{(t)} \in \{0, 1\}$. As explained in Sec. I, we consider a potentially heterogeneous detection setting, where the channel may be occupied by primary users in a certain location and free in another location. This is the case of *spectrum holes in space*, as discussed in [16]. The extent of a spectrum hole in space is determined by the transmit power and communication range of primary users, or by the presence of physical barriers (e.g., walls).

The time is modeled as slotted. At each time slot, secondary users perform spectrum sensing by measuring the average energy, $\frac{1}{N}\|\mathbf{y}_k^{(t)}\|^2$, where $\mathbf{y}_k^{(t)} \triangleq \left[y_k^{(t)}(1), \ldots, y_k^{(t)}(N)\right]$ is a vector of N complex base-band received signal samples. Depending on $\mathcal{H}_k^{(t)}$, the generic sample can be written as

$$y_k^{(t)}(n) = \begin{cases} v_k(n) & \text{if} \quad \mathcal{H}_k^{(t)} = 0, \\ x_k(n) + v_k(n) & \text{if} \quad \mathcal{H}_k^{(t)} = 1, \end{cases} \quad (1)$$

where $v_k(n) \sim \mathcal{N}(0, \sigma_v^2)$ is complex white Gaussian noise, and $x_k(n)$ represents the signal received from a primary user

if active. Signals are modeled as zero-mean random variables with $\mathbb{E}|x_k(n)|^2 \triangleq \sigma_k^2$, which includes the channel gain. The signal-to-noise ratio (SNR) at node k is defined as

$$\rho_k \triangleq \frac{\sigma_k^2}{\sigma_v^2}. \quad (2)$$

B. Single Node Detection

Since hypotheses $\mathcal{H}_k^{(t)}$ may be different for different nodes and at different time slots, the most general approach is obtained assuming all sensors as independent and performing signal detection separately at each single node and time slot. In this perspective, the test statistic available at node k is the vector $\mathbf{y}_k^{(t)}$. Assuming the received signal samples as complex Gaussian distributed (which is a reasonable approximation for practical modulated signals, taking into account the effects of fast fading and non-coherent reception), the single-sensor likelihood ratio test (LRT) is given by

$$\begin{aligned} L_k^{(t)} &\triangleq \frac{p(\mathbf{y}_k^{(t)}|\mathcal{H}_k^{(t)} = 1)}{p(\mathbf{y}_k^{(t)}|\mathcal{H}_k^{(t)} = 0)} \quad (3) \\ &= \frac{(\sigma_v^2)^{N-1}}{1 + \rho_k} \exp\left(\frac{\|\mathbf{y}_k^{(t)}\|^2}{\sigma_v^2} \frac{\rho_k}{1 + \rho_k}\right) \underset{\hat{\mathcal{H}}_k^{(t)}=0}{\overset{\hat{\mathcal{H}}_k^{(t)}=1}{\gtrless}} \tau. \quad (4) \end{aligned}$$

The above LRT can be seen from two points of view: as a Bayesian test, if the prior distributions of $\mathcal{H}_k^{(t)}$ and of $\mathbf{y}_k^{(t)}$ are uniform (non-informative); or as a NP test, in which case the threshold τ is chosen as a function of the desired false alarm rate α. From (4) it follows that the energy $\frac{1}{N}\|\mathbf{y}_k^{(t)}\|^2$ is a sufficient statistic for the LRT, i.e., energy detection is optimal in case of single-sensor detection. Thus, taking logarithms on both sides of L_k, we can rewrite the test as

$$\frac{1}{N}\|\mathbf{y}_k^{(t)}\|^2 \underset{\hat{\mathcal{H}}_k^{(t)}=0}{\overset{\hat{\mathcal{H}}_k^{(t)}=1}{\gtrless}} \eta \quad (5)$$

with

$$\eta \triangleq \frac{\sigma_v^2}{N}\left(1 + \frac{1}{\rho_k}\right)\left[\log(1 + \rho_k) + \log\tau - (N-1)\log\sigma_v^2\right]. \quad (6)$$

If the NP approach is adopted, the new threshold η needs not be computed from τ, but it is chosen such that $\Pr\left(\frac{1}{N}\|\mathbf{y}_k^{(t)}\|^2 > \eta \big| \mathcal{H}_k^{(t)} = 0\right) = \alpha$, which yields

$$\eta(\alpha) = \sigma_v^2\left[1 + N^{-1/2}Q^{-1}(\alpha)\right], \quad (7)$$

as follows from well-known results on energy detection (cf. [17], [18]).

We then define for each node an *individual observation factor*

$$F_k^{(t)} \triangleq \frac{1}{N}\|\mathbf{y}_k^{(t)}\|^2 - \eta(\alpha) \underset{\hat{\mathcal{H}}_k^{(t)}=0}{\overset{\hat{\mathcal{H}}_k^{(t)}=1}{\gtrless}} 0. \quad (8)$$

Note that the above statistics have the form of log-likelihood ratio (LLR) tests. We also remark that, thanks to the adoption of a NP approach, factors F_k only require knowledge of the noise variance (which can be estimated as the average energy of no-signal slots, offline or online) but not of the SNR of the signal to be detected. On the contrary, Bayesian likelihood

ratios (e.g., [14], [15]) require prior knowledge of the SNR under hypothesis $\mathcal{H} = 1$ and lack a general analytic method to set the decision threshold as a function of the false-alarm rate.

C. Statistical Dependencies

Single-user detection is optimal only when all sensors are uncorrelated. In realistic scenarios, it is likely that some correlation exists between the channel occupancy of neighboring nodes [14], [19], although such correlation is *a priori* unknown and may be time-varying (e.g., due to mobile primary users, changes in the radio environment, etc.). We propose to take into account this condition through a *pairwise Markov random field (MRF)* model [20]. As such, we introduce a joint prior distribution of variables $\mathcal{H}_k^{(t)}$ in the form of a product of pairwise exponential terms:

$$p(\mathcal{H}_1^{(t)}, \ldots, \mathcal{H}_K^{(t)}) = \frac{1}{Z} \prod_{\substack{j \in \mathcal{N}_k \\ k < j}} \exp\left(\lambda \Delta_{kj}^{(t)} \cdot \mathbf{1}\{\mathcal{H}_k^{(t)} = \mathcal{H}_j^{(t)}\}\right),$$

$$(9)$$

where $\mathcal{N}_k$ is the set of nodes within the communication range of k ("neighbors"), Z is a normalization constant such that the probability sums to 1, $\lambda < 1$ is a small positive constant, $\mathbf{1}\{x\} = 1$ if x is true or 0 otherwise, and $\Delta_{kj}^{(t)}$ is learned from a number T of previous time slots as follows:

$$\Delta_{kj}^{(t)} \triangleq \sum_{q=t-T}^{t-1} \mathbf{1}\{\hat{\mathcal{H}}_k^{(q)} = \hat{\mathcal{H}}_j^{(q)}\} - \mathbf{1}\{\hat{\mathcal{H}}_k^{(q)} \neq \hat{\mathcal{H}}_j^{(q)}\}. \quad (10)$$

In practice, $\Delta_{kj}^{(t)}$ can be updated recursively by

$$\Delta_{kj}^{(t)} = \Delta_{kj}^{(t-1)} + \mathbf{1}\{\hat{\mathcal{H}}_k^{(t-1)} = \hat{\mathcal{H}}_j^{(t-1)}\} - \mathbf{1}\{\hat{\mathcal{H}}_k^{(t-1)} \neq \hat{\mathcal{H}}_j^{(t-1)}\}.$$

$$(11)$$

The rationale for the proposed model is the following: the exponential terms in (9) assign higher probability to the event of nodes k and j having the same state $\mathcal{H}_k^{(t)} = \mathcal{H}_j^{(t)}$, if the decisions of nodes k and j have been equal in the majority of previous observations. The strength of interconnection between $\mathcal{H}_k^{(t)}$ and $\mathcal{H}_j^{(t)}$ is adjusted by the product $\lambda \Delta_{kj}$. Since $-T < \Delta_{kj} < T$, the constant λ should be chosen such that $\exp(\lambda T) \gg 1$, i.e., a large number of equal decisions between nodes k and j results in a high probability of $\mathcal{H}_k^{(t)}$ and $\mathcal{H}_j^{(t)}$ being equal. On the other hand, if $|\Delta_{kj}|$ is small (no significant correlation between previous decisions of nodes k and j), then $\exp(\lambda \Delta_{kj}) \approx 1$, i.e., the MRF distribution becomes non-informative.

D. Resulting Model

By combining the prior MRF joint distribution with individual observation likelihoods, we can express the joint *a posteriori* distribution of variables $\mathcal{H}_1^{(t)}, \ldots, \mathcal{H}_K^{(t)}$ as

$$p(\mathcal{H}_1^{(t)}, \ldots, \mathcal{H}_K^{(t)} | \mathbf{y}_1^{(t)}, \ldots, \mathbf{y}_K^{(t)}) \propto \prod_{k=1}^{K} p(\mathbf{y}_k^{(t)} | \mathcal{H}_k^{(t)}) \times$$

$$\prod_{\substack{j \in \mathcal{N}_k \\ k < j}} \exp\left(\lambda \Delta_{kj}^{(t)} \cdot \mathbf{1}\{\mathcal{H}_k^{(t)} = \mathcal{H}_j^{(t)}\}\right). \quad (12)$$

Note that, if $p(\mathcal{H}_k^{(t)})$ is uniform, then $p(\mathbf{y}_k^{(t)} | \mathcal{H}_k^{(t)})$ and $p(\mathcal{H}_k^{(t)} | \mathbf{y}_k^{(t)})$ are equivalent up to a proportionality constant. Then, the signal detection problem for every node k can be formulated as a LRT of the marginal a posteriori probabilities,

$$L_k^{\text{post}} \triangleq \frac{p(\mathcal{H}_k^{(t)} = 1 | \mathbf{y}_1^{(t)}, \ldots, \mathbf{y}_K^{(t)})}{p(\mathcal{H}_k^{(t)} = 0 | \mathbf{y}_1^{(t)}, \ldots, \mathbf{y}_K^{(t)})}, \quad (13)$$

with

$$p(\mathcal{H}_k^{(t)} | \mathbf{y}_1^{(t)}, \ldots, \mathbf{y}_K^{(t)}) = \sum_{\sim \{\mathcal{H}_k^{(t)}\}} p(\mathcal{H}_1^{(t)}, \ldots, \mathcal{H}_K^{(t)} | \mathbf{y}_1^{(t)}, \ldots, \mathbf{y}_K^{(t)})$$

$$(14)$$

where the notation $\sum_{\sim \{\mathcal{H}_k^{(t)}\}}$ denotes multiple summation over all variables $\{\mathcal{H}_1^{(t)}, \ldots, \mathcal{H}_K^{(t)}\}$ except $\mathcal{H}_k^{(t)}$.

We next introduce a decentralized algorithm which, through an iterative exchange of local messages between network nodes, approximates the marginal LRTs of interest (13) while at the same time setting constraints on the local false-alarm probabilities for each node, in a NP-like fashion. A summary of the notation used throughout the paper is provided in Tab. I.

III. MESSAGE PASSING ALGORITHM

In order to estimate the marginal LRTs, we apply the sum-product algorithm over factor graphs [21] to the model defined by Eq. (12). In our model, each factor is connected to at most two variables, therefore we can express message update rules directly from one variable to another. Note that a decentralized implementation of the BP algorithm is enabled by the one-to-one correspondence between variables $\mathcal{H}_k^{(t)}$ and nodes in the network. As such, a generic message from node k to node j at iteration l is given by

$$\mu_{k \to j}^{(t,l)}(\mathcal{H}_j^{(t)}) \propto \sum_{\mathcal{H}_k^{(t)} \in \{0,1\}} \left(p(\mathbf{y}_k^{(t)} | \mathcal{H}_k^{(t)}) \times \right. \quad (15)$$

$$\left. \exp(\lambda \Delta_{kj}^{(t)} \cdot \mathbf{1}\{\mathcal{H}_k^{(t)} = \mathcal{H}_j^{(t)}\}) \prod_{n \in \mathcal{N}_k \setminus \{j\}} \mu_{n \to k}^{(t,l-1)}(\mathcal{H}_k^{(t)}) \right).$$

Messages at iteration $l = 0$ are initialized as uniform distributions. Beliefs, i.e., estimates of the marginal probabilities (14), are computed at each iteration l as

$$b_k^{(t,l)}(\mathcal{H}_k^{(t)}) \propto \prod_{n \in \mathcal{N}_k} \mu_{n \to k}^{(t,l)}(\mathcal{H}_k^{(t)}). \quad (16)$$

The proportionality sign in (15) and (16) indicates that beliefs and messages are expressed up to a constant, which can be found by normalizing $b(\cdot)$ and $\mu(\cdot)$ so as to sum to 1.

We now express message update rules in terms of LLRs. We define LLR beliefs

$$\Lambda_k^{(t,l)} \triangleq \log \frac{b_k^{(t,l)}(\mathcal{H}_k^{(t)} = 1)}{b_k^{(t,l)}(\mathcal{H}_k^{(t)} = 0)} \quad (17)$$

and messages

$$M_{k \to j}^{(t,l)} \triangleq \log \frac{\mu_{k \to j}^{(t,l)}(\mathcal{H}_j^{(t)} = 1)}{\mu_{k \to j}^{(t,l)}(\mathcal{H}_j^{(t)} = 0)}. \quad (18)$$

TABLE I
SUMMARY OF SYMBOLS USED IN THE PAPER AND THEIR MEANING.

Symbol	Definition	Meaning
$\|\mathbf{a}\|^2$	$\sum_{i=1}^{N}\|a_i\|^2$	Euclidean squared norm of a vector $\mathbf{a} \in \mathbb{C}^n$
$\mathcal{H}_k^{(t)}$	$\in \{0,1\}$	Channel occupation of user k at time slot t
$\mathbf{y}_k^{(t)}$	–	Received signal vector (N samples) of user k at time slot t
$L_k^{(t)}$	$\frac{p(\mathbf{y}_k^{(t)}\|\mathcal{H}_k^{(t)}=1)}{p(\mathbf{y}_k^{(t)}\|\mathcal{H}_k^{(t)}=0)}$	Individual likelihood ratio
$F_k^{(t)}$	$\frac{1}{N}\|\mathbf{y}_k^{(t)}\|^2 - \eta(\alpha)$	Individual observation factor
$\eta(\alpha)$	$\sigma_v^2\left[1 + N^{-1/2}Q^{-1}(\alpha)\right]$	Decision threshold for false-alarm rate α
$Q(x)$	$\frac{1}{\sqrt{2\pi}}\int_x^{\infty} e^{-t^2/2}dt$	Gaussian tail function
$\mathcal{N}_k$	–	Set of neighboring nodes of k
$\mathbf{1}\{x\}$	1 if x is true, 0 otherwise	Indicator function
λ	$0 < \lambda < 1$	Learning factor (constant)
$\Delta_{ij}^{(t)}$	Eq. (10)	Strength of interaction between nodes i and j (learned)
L_k^{post}	$\frac{p(\mathcal{H}_k^{(t)}=1\|\mathbf{y}_1^{(t)},\ldots,\mathbf{y}_K^{(t)})}{p(\mathcal{H}_k^{(t)}=0\|\mathbf{y}_1^{(t)},\ldots,\mathbf{y}_K^{(t)})}$	A posteriori likelihood ratio
$\mathcal{S}(a,b)$	$\log\frac{1+e^{a+b}}{e^a+e^b}$	$\mathcal{S}$-function used in message computation
$\mu_{k\to j}^{(t,l)}, b_k^{(t,l)}$	Eqs. (15,16)	Messages/beliefs at time t, iteration l (probability domain)
$M_{k\to j}^{(t,l)}, \Lambda_k^{(t,l)}$	Eqs. (17,18)	Messages/beliefs at time t, iteration l (LLR domain)
r_{kj}	$\frac{\mathbb{E}\left[(\mathcal{H}_k-\mu_k)(\mathcal{H}_j-\mu_j)\right]}{\sigma_k\sigma_j}$	Statistical correlation between $\mathcal{H}_k$ and $\mathcal{H}_j$
$\mathcal{C}$	$\{k : \mathcal{H}_k = 0\ \forall k\ \text{or}\ \mathcal{H}_k = 1\ \forall k\}$	Cluster (set of nodes under homogeneous radio conditions)
$\eta_{\mathcal{C}}(\alpha)$	$\sigma_v^2\left[1 + (\|\mathcal{C}\|N)^{-1/2}Q^{-1}(\alpha)\right]$	Decision threshold taking cooperation into account

After algebraic manipulations, we can rewrite message and belief update rules in LLR form as

$$M_{k\to j}^{(t,l)} = \mathcal{S}\left(\lambda\Delta_{kj}^{(t)}, \ \log L_k^{(t)} + \sum_{n\in\mathcal{N}_k\setminus\{j\}} M_{n\to k}^{(t,l-1)}\right), \quad (19)$$

$$\Lambda_k^{(t,l)} = \log L_k^{(t)} + \sum_{n\in\mathcal{N}_k} M_{n\to k}^{(t,l)}, \quad (20)$$

where

$$\mathcal{S}(a,b) \triangleq \log\frac{1+e^{a+b}}{e^a+e^b}, \quad (21)$$

and $L_k^{(t)}$ is given by (3). As explained in Sec. II-B, expressing $L_k^{(t)}$ in explicit form requires knowledge of the distribution of $\mathbf{y}_k^{(t)}$ under the hypothesis of signal present, which ultimately amounts to the knowledge of the SNR ρ_k. Furthermore, even assuming a prior knowledge, or guess, of the signal strength, the problem of setting the decision threshold τ remains unsolved: if one assigns equal weights to type-I and type-II errors (false alarms and missed detections), then the threshold should be set to 1 (i.e., 0 in the LLR domain), but this approach is not useful to ensure a false-alarm rate lower than a specified value.

On the other hand, we have shown in Sec. II-B that the LRT on $L_k^{(t)}$ is equivalent to a LLR test of the energy $\frac{1}{N}\|\mathbf{y}_k^{(t)}\|^2$ against a modified threshold $\eta(\alpha)$ that can be expressed directly as a function of the false-alarm rate. Therefore, we set

$$\log L_k^{(t)} := F_k^{(t)} = \frac{1}{N}\|\mathbf{y}_k^{(t)}\|^2 - \eta(\alpha) \quad (22)$$

in (19) and (20), with $F_k^{(t)}$ defined in (8). In this way we have applied a combined NP-Bayesian methodology to the multi-sensor detection problem: individual observations are processed by a NP approach, which is insensitive to SNR knowledge and offers control over the false-alarm rate, and

are reinforced by peer-to-peer collaboration, implemented by means of a Bayesian joint prior distribution estimated from previous time slots.

After a sufficient number of iterations (l^*), each node makes a decision on $\mathcal{H}_k^{(t)}$ simply based on the sign of its LLR belief:

$$\Lambda_k^{(t,l^*)} \underset{\hat{\mathcal{H}}_k^{(t)}=0}{\overset{\hat{\mathcal{H}}_k^{(t)}=1}{\gtrless}} 0. \quad (23)$$

Observe that the threshold on beliefs is set to zero as a result of (8). This implies that for each node the achieved false-alarm probability is always equal to α (in case of no correlation with neighbors) or lower. More details about this property are given in Sec. IV.

The graphical model is illustrated in Fig. 1 for a simple network of $K = 3$ nodes. Since all factors are pairwise, we represent factors simply as edges in the graph, and variables as vertices. This representation allows an intuitive mapping between graphical model and physical network. The figure shows the intrinsic information of each node, F_k, which can interpreted as a factor connected to a single variable, and messages $M_{k\to j}$ exchanged in the network at a certain iteration and time slot.

The resulting algorithm, called *NP-BP*, is summarized in Alg. 1. From the point of view of implementation it is worth noting that messages defined in LLR form are scalar numbers, which can be represented using few bits in the packets that are exchanged in the network. Finally, the number of iterations needed to reach convergence of the algorithm depends, in general, on the size and on the structure of the "clusters" of the network, i.e., the groups of nodes under the same hypothesis. It is observed empirically that very few iterations (e.g., 3) are enough to reach convergence (at least of final decisions, i.e., binary beliefs) even in large-scale networks.
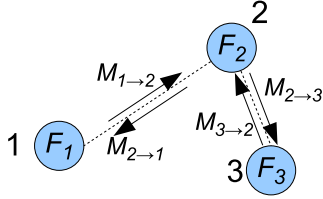
Fig. 1. Graphical model for a simple network of 3 nodes, representing messages and individual likelihood functions at a certain time slot t and iteration l. The statistical graph matches with the network topology, therefore messages can be exchanged by nodes in a decentralized fashion.

Algorithm 1: Decentralized NP-BP algorithm

Input : Number of iterations l^*; false alarm rate α; max. number of time slots used for learning $T_{\max}$; constant λ.

Output: Decisions $\{\hat{\mathcal{H}}_k^{(1)}, \ldots, \hat{\mathcal{H}}_k^{(S)}\} \; \forall k \in \{1, \ldots, K\}$.

1 **for** *time slot $t = 1$ to S* **do**
2   Set $T = \min\{t, T_{\max}\}$;
3   **for** *nodes $k \in \{1, \ldots, K\}$* **do**
4   **for** *neighbors $j \in \mathcal{N}_k$* **do**
5   **if** $k < j$ **then**
6   Update $\Delta_{kj}^{(t)}$ using (10);
7   **else**
8                   $\Delta_{kj}^{(t)} = \Delta_{jk}^{(t)}$;
9   **end**
10   **end**
11   **end**
12   **for** *nodes $k \in \{1, \ldots, K\}$* **in parallel do**
13   Collect N received signal samples, $\mathbf{y}_k^{(t)}$;
14   Compute $F_k^{(t)}$ from (8);
15   Initialize and broadcast $M_{k \to j}^{(t,0)} = 0 \; \forall j \in \mathcal{N}_k$;
16   **for** *iteration $l = 1$ to l^** **do**
17   Receive incoming messages from neighbors: $M_{n \to k}^{(t,l-1)} \; \forall n \in \mathcal{N}_k$;
18   **for** *nodes $j \in \mathcal{N}_k$* **do**
19   Compute outgoing message $M_{k \to j}^{(t,l)}$ from (19) and send it to node j;
20   **end**
21   **end**
22   Compute belief $\Lambda_k^{(t,l^*)}$ from (20);
23   Make decision $\hat{\mathcal{H}}_k^{(t)}$ using (23);
24   **end**
25 **end**

IV. PERFORMANCE ANALYSIS

In this section we investigate the performance of the proposed NP-BP method. First of all, we observe that, for sufficiently large T, the quantity $\Delta_{kj}^{(t)}$ defined in (10) is directly related to the correlation r_{kj} between variables $\mathcal{H}_k$ and $\mathcal{H}_j$[2]:

$$r_{kj} > 0 \quad \Leftrightarrow \quad \Delta_{kj}^{(t)} \to \infty \tag{24}$$

$$r_{kj} = 0 \quad \Leftrightarrow \quad \Delta_{kj}^{(t)} \to 0 \tag{25}$$

$$r_{kj} < 0 \quad \Leftrightarrow \quad \Delta_{kj}^{(t)} \to -\infty. \tag{26}$$

---

[2]The correlation coefficient is defined as $r_{kj} \triangleq \frac{\mathbb{E}[(\mathcal{H}_k - \mu_k)(\mathcal{H}_j - \mu_j)]}{\sigma_k \sigma_j} = \frac{\mathbb{E}[\mathcal{H}_k \mathcal{H}_j] - 0.25}{0.25}$. The index t is dropped as $\mathcal{H}_k$ and $\mathcal{H}_j$ are considered here as random variables, of which $\mathcal{H}_k^{(t)}$ and $\mathcal{H}_j^{(t)}$ are realizations at time t.
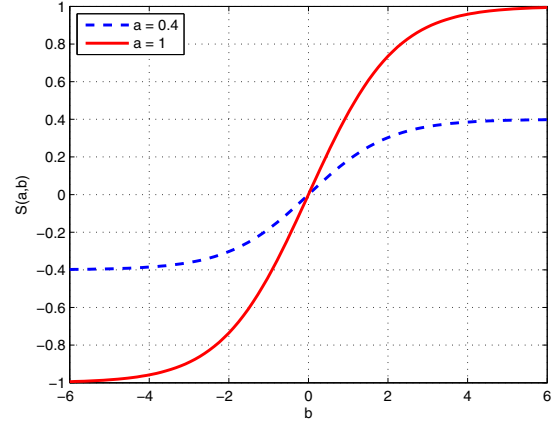

Fig. 2. Plot of $\mathcal{S}(a, b)$ for different values of a.

The first case includes in particular $r_{kj} = 1$, which means $\mathcal{H}_k = \mathcal{H}_j$ (two nodes under the same hypothesis). The second case represents nodes that observe uncorrelated data, for example activity from different primary users. The third case occurs if two nodes remain under opposite hypotheses for long time.

Having established a relation between the learned parameter $\Delta_{kj}^{(t)}$ and the statistical correlation r_{kj}, an asymptotic performance analysis of the NP-BP algorithm will be developed next (Sec. IV-A) for two opposite correlation regimes: uncorrelated nodes and highly correlated nodes. The analysis of the dynamics of BP, which is very complex in general (see, e.g., [30], [32]), is considerably simplified under the above limiting conditions. Nevertheless, the results derived for these simple cases give insight into the performance of the NP-BP algorithm in conditions of most practical interest.

Before moving forward, it is useful to analyze the asymptotic behavior of the function $\mathcal{S}(a, b)$ defined by (21). We note that: *(i)* $\mathcal{S}(a, b)$ is symmetric with respect to its arguments, a and b; *(ii)* when one of the arguments is significantly larger than the other one, the function tends to $\min\{a, b\}$. The function $\mathcal{S}(a, b)$ is plotted in Fig. 2 for different values of the parameters. In the message update rule (19), the first argument is $\lambda \Delta_{kj}^{(t)}$, i.e., a quantity that grows with the number of available previous observations when these reveal correlation with neighboring nodes; the second argument is the sum of the neighbor's individual likelihood ratio and incoming messages.

A. Asymptotic Analysis

We can identify two extreme operating conditions of NP-BP. For each case, we first express a generic message between two neighboring nodes k and j, and then the belief of a generic node k.

1) *No available past observations* or *no correlation between nodes k and j*: $\lambda \Delta_{kj}^{(t)} \ll F_k^{(t)}$. In this case, from (19) we have

$$M_{k \to j}^{(t,l)} \approx \lambda \Delta_{kj}^{(t)}. \tag{27}$$

Then, assuming that a node k is uncorrelated from its neighbors $n \in \mathcal{N}_k$, we obtain from (20)

$$\Lambda_k^{(t,l^*)} \approx F_k^{(t)} + \lambda \sum_{n \in \mathcal{N}_k} \Delta_{nk}^{(t)}. \tag{28}$$

Since λ is a small constant (typically $\ll 1$) and, in absence of correlation between nodes, $\Delta_{nk}^{(t)} \approx 0$ (25), Eq. (28) reduces to $\Lambda_k^{(t,l)} \approx F_k^{(t)}$. Note that this approximation is motivated not only for long observation periods (large T), but also for small T, because by definition $\lambda \Delta_{nk}^{(t)}$ takes significant values only after a certain number of time slots. In addition, if there are enough neighbors having no correlation with k, the sign of $\Delta_{nk}^{(t)}$ is positive or negative with equal probability, hence the sum tends to zero.

As a result, in absence of correlation, the proposed spectrum sensing procedure *reduces to single-user energy detection*: each node separately tests $F_k^{(t)} \gtrless 0$, which is equal to $\frac{1}{N}\|\mathbf{y}_k^{(t)}\|^2 \gtrless \eta(\alpha)$. This property guarantees that the average false-alarm rate achieved by each node is, in the worst case (no cooperation among nodes), equal to α, thus satisfying the Neyman-Pearson requirement of an upper bound to the false-alarm rate. In case of a sudden change in the radio environment that makes two previously correlated nodes (k, j) become uncorrelated, the system automatically learns the new situation within a few time slots thanks to the update of $\Delta_{kj}^{(t)}$ (10). The learning rate is determined by the coefficient λ: lower λ results in a slower adaptation and more conservative use of neighbors' data; higher λ makes the system more reactive to changes, but may result in overconfident estimation of correlations with neighbors. The optimization of λ is a subject beyond the scope of this paper. Empirically, the value of $\lambda = 0.1$ was chosen and used in simulations (see Sec. V).

2) *Significant correlation between nodes k and j*: $\lambda \Delta_{kj}^{(t)} \gg F_k^{(t)}$. In this case, (19) becomes

$$M_{k \to j}^{(t,l)} \approx F_k^{(t)} + \sum_{n \in \mathcal{N}_k \backslash \{j\}} M_{n \to k}^{(t,l-1)}. \qquad (29)$$

Applied iteratively, the above expression leads to formation of *clusters* of nodes correlated with each other: after a number of iterations L sufficient to span the entire cluster, the test statistic of each node in the cluster converges to the sum of individual LLR functions of all such nodes. More formally, let $\mathcal{C}$ be a set of nodes under the same hypothesis $\mathcal{H}_k^{(t)} = 0$ or $\mathcal{H}_k^{(t)} = 1 \; \forall k \in \mathcal{C}$. If the state $\mathcal{H}_k^{(t)}$ does not change for a sufficient number of consecutive time slots, $\Delta_{kj}^{(t)}$ increases and the condition $\lambda \Delta_{kj}^{(t)} \gg F_k^{(t)}$ is eventually satisfied for all nodes $k \in \mathcal{C}$. Hence, for any $k \in \mathcal{C}$,

$$\Lambda_k^{(t,l^*)} \approx \sum_{k \in \mathcal{C}} F_k^{(t)} = |\mathcal{C}| \left(\frac{1}{|\mathcal{C}|N} \sum_{k \in \mathcal{C}} \|\mathbf{y}_k^{(t)}\|^2 - \eta(\alpha) \right), \qquad (30)$$

where $|\mathcal{C}|$ is the cardinality of $\mathcal{C}$, i.e., the number of nodes in the cluster. Hence, the test for any $k \in \mathcal{C}$ can be rewritten as

$$\frac{1}{|\mathcal{C}|N} \sum_{k \in \mathcal{C}} \|\mathbf{y}_k^{(t)}\|^2 \underset{\hat{\mathcal{H}}_k^{(t)}=0}{\overset{\hat{\mathcal{H}}_k^{(t)}=1}{\gtrless}} \eta(\alpha) \qquad (31)$$

and is equivalent to *cooperative energy detection (CED)* by all nodes in the cluster. Note that the beliefs of all nodes $k \in \mathcal{C}$ converge to the same test statistic (31), therefore the NP-BP algorithm can be interpreted (for highly correlated nodes) as a cluster-wise consensus scheme.

B. Comparison to Centralized Cooperative Energy Detection Approaches

CED has been extensively studied in the spectrum sensing literature. Examples of different CED approaches can be found in [25]–[29], all assuming a centralized architecture.

A first distinction can be made between *soft-decision* and *hard-decision* fusion schemes. In the first case, every sensor sends the measured energy value to the fusion center, while in the second case it sends only one bit representing the sensor's local decision. Intermediate versions (e.g., 2-bit quantization) are presented in [27]. Clearly, hard-decision is suboptimal compared to soft-decision, but requires less bandwidth.

CED algorithms can be further divided based on the weights assigned to different sensors. If the measurements from all sensors are equally weighted, we refer to *equal gain combining (EGC)* schemes. In [26], an optimization procedure for the weighting coefficients is proposed. *Maximal ratio combining (MRC)* schemes, where weights are proportional to local SNRs ρ_k, are presented in [25], [27]. Then, in [27], the *optimal combining (OC)* scheme in the Neyman-Pearson sense for soft energy measurements is shown to be

$$T_{OC} = \sum_k \frac{\rho_k}{1 + \rho_k} \|\mathbf{y}_k^{(t)}\|^2. \qquad (32)$$

According to the above classification, the scheme proposed in this paper can be interpreted as a decentralized, cluster-wise *CED-EGC soft-decision scheme* (31). Note that a CED-OC scheme equivalent to (32) can be obtained in the NP-BP framework as well, by including coefficients $\frac{\rho_k}{1+\rho_k}$, which appear in (4), into $F_k^{(t)}$ (8). However, since exact knowledge of the SNRs ρ_k is difficult to obtain in a decentralized cognitive radio setting, all results presented in this paper refer to the EGC case.

From an architectural point of view, the advantage of the NP-BP method compared to centralized CED is that cooperation is achieved in a fully decentralized way, without a fusion center like in traditional cooperative spectrum sensing approaches. In addition, the proposed method does not require prior knowledge of the nodes participating in cooperative detection, because clustering is determined automatically based on the evolution of coefficients $\Delta_{kj}^{(t)}$. The above properties ensure robustness and scalability of the sensing algorithm. From the point of view of performance, the gain is twofold: *(i)* NP-BP is able to iteratively fuse data from nodes that are more than one-hop away (*multi-hop gain*); *(ii)* thanks to the learning procedure, each node performs a selective data fusion, i.e., only measurements from neighbors under similar radio conditions are considered (*clustering gain*). The resulting performance improvement is illustrated by simulation results in Sec. V.

We finally remark that the the concept of clustering is not new in the literature of spectrum sensing. However, previous works such as [28], [29] consider clustering as a way to reduce the number of messages exchanged between the sensors

and the fusion center (still in a centralized architecture), by selecting only the most representative node of each cluster. Our approach, on the contrary, introduces clustering as a way to cope with heterogeneous radio conditions and to enable identification of local spectrum holes (see also [14], [18]).

C. False-alarm Probability and Selection of the Threshold

1) Single-user threshold: The threshold $\eta(\alpha)$ given by (7) is tailored for the single-user case. Clearly, if a node has no collaborating neighbors, the resulting false-alarm probability is $P_{\text{fa}} = \alpha$. However, cooperation among multiple nodes provides an improvement of the false-alarm probability at a given threshold: if all nodes in $\mathcal{C}$ are under the same condition ($\mathcal{H} = 0$), the resulting false-alarm probability is

$$P_{\text{fa}}(\mathcal{C}) = Q\left[\sqrt{|\mathcal{C}|N}\left(\frac{\eta}{\sigma_v^2} - 1\right)\right], \qquad (33)$$

as in an energy detector with $|\mathcal{C}|N$ samples. Therefore, setting η as (7) in the cooperative case gives a false-alarm rate lower than the nominal value α.

2) Cooperative threshold: In case of cooperation, a new threshold

$$\eta_{\mathcal{C}}(\alpha) = \sigma_v^2\left[1 + (|\mathcal{C}|N)^{-1/2}Q^{-1}(\alpha)\right] \qquad (34)$$

can be then computed from inversion of (33), resulting exactly in $P_{\text{fa}}(\mathcal{C}) = \alpha$ for all $k \in \mathcal{C}$. The new "cooperative" threshold can be set once clusters are established with sufficient stability, and the number of nodes in the cluster ($|\mathcal{C}|$) must be constantly verified based on coefficients $\Delta_{kj}^{(t)}$. Note that such a threshold selection may fail to guarantee the required false-alarm rate in case of changes in the radio environment for the nodes in $\mathcal{C}$. However, thanks to the automatic update of coefficient $\Delta_{kj}^{(t)}$, normal conditions are restored within a few time slots.

D. Detection Performance

The resulting detection probability for a cluster $\mathcal{C}$ can be computed again by using results from energy detection theory (cf. [17], [18]). From (31), the test statistic can be written as

$$T_{\mathcal{C}} \triangleq \frac{1}{|\mathcal{C}|N}\sum_{k\in\mathcal{C}}\|\mathbf{y}_k^{(t)}\|^2 = \frac{1}{|\mathcal{C}|}\sum_{k\in\mathcal{C}}T_k, \qquad (35)$$

and $T_k \sim \mathcal{N}\left(1 + \overline{\rho}_{\mathcal{C}}, \frac{1}{|\mathcal{C}|^2N}\sum_{k\in\mathcal{C}}(1 + \rho_k)^2\right)$, with $\overline{\rho}_{\mathcal{C}} \triangleq \frac{1}{|\mathcal{C}|}\sum_{k\in\mathcal{C}}\rho_k$, by linearity of the normal distribution. Hence, the detection probability is

$$P_{\text{d}}(\mathcal{C}) = \Pr[T_{\mathcal{C}} > \eta] = Q\left(|\mathcal{C}|\sqrt{N}\frac{\eta/\sigma_v^2 - 1 - \overline{\rho}_{\mathcal{C}}}{\sqrt{\sum_{k\in\mathcal{C}}(1 + \rho_k)^2}}\right). \qquad (36)$$

If all nodes in $\mathcal{C}$ are under the same SNR ρ, the above formula reduces to

$$P_{\text{d}}(\mathcal{C}) = Q\left[\sqrt{|\mathcal{C}|N}\left(\frac{\eta/\sigma_v^2}{1 + \rho} - 1\right)\right], \qquad (37)$$

which is the same performance of a single energy detector with $|\mathcal{C}|N$ samples, similarly as in (33).

Note that, if a node has no cooperating neighbors, the same result (37) holds with $|\mathcal{C}| = 1$ thus reducing to traditional single-user energy detection.

E. Impact of Cycles in the Graph

Convergence and performance of the proposed algorithm may be affected by the presence of cycles in the statistical graph, which in turn depends on the network topology and the communication range of nodes. It is known that BP may not converge to the true posterior probabilities in case of "loopy" graphs. In [30] it was shown that, due to cycles, beliefs tend to be overconfident, because the same piece of information may reach a node through multiple paths. In [31], [32], we have proposed a simple method, named "uniformly reweighted (URW) BP", able to mitigate this problem while admitting a decentralized implementation. In URW-BP, messages are weighted by a constant $\epsilon \in (0,1)$, which represents the average appearance probability of edges in the graph.

In the considered application, URW-BP message and belief update rules – cf. (19), (20) – are given by

$$M_{k\to j}^{(t,l)} = \mathcal{S}\left(\frac{\lambda\Delta_{kj}^{(t)}}{\varepsilon}, \; \log L_k^{(t)} + (\varepsilon - 1)M_{j\to k}^{(t,l-1)}\right. \qquad (38)$$
$$\left. + \; \varepsilon \sum_{n\in\mathcal{N}_k\setminus\{j\}} M_{n\to k}^{(t,l-1)}\right),$$

$$\Lambda_k^{(t,l)} = \log L_k^{(t)} + \varepsilon \sum_{n\in\mathcal{N}_k} M_{n\to k}^{(t,l)}, \qquad (39)$$
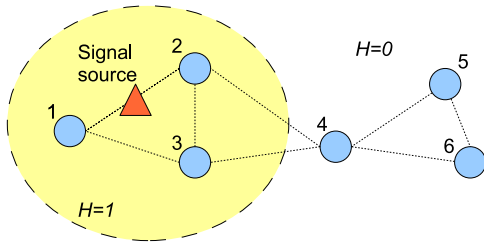
with

$$\varepsilon \triangleq \min(1, \; 2/n_D), \qquad (40)$$

where n_D is the average degree of the graph, i.e., the average number of connections of the nodes in the network. Note that n_D can be computed in a decentralized architecture by an average consensus algorithm [33].

We remark that there is no need to apply URW-BP when the number of iterations is small (more precisely: lower than the size of cycles in the graph). In this case, messages do not propagate long enough to affect the performance of standard BP. On the other hand, if the number of iterations is larger than the loop size, URW-BP is able to provide a significant performance improvement over BP, as shown in the next section.

F. Complexity

The computational complexity of NP-BP is very low, since in the adopted LLR representation all messages are scalar quantities, and their computation only involves sums and products. From a networking point of view, the main issue is message exchange, because *(i)* messages occupy some bandwidth (although limited), and *(ii)* packet transmission may fail and require retransmission(s). The latter problem is particularly relevant if nodes communicate over the same wireless channel that they are sensing, and that is possibly occupied by a primary user. In order to minimize both bandwidth usage and transmission errors, it is convenient to reduce the number of iterations of NP-BP. As an example, simulation results shown in the next section demonstrate that 3 iterations per time slot already provide excellent performance in all considered scenarios.

(a) Small-scale network ($K = 6$ nodes). 3 nodes are under $\mathcal{H} = 1$, 3 under $\mathcal{H} = 0$. Each node can communicate with its neighbors; connections are indicated by dotted lines.
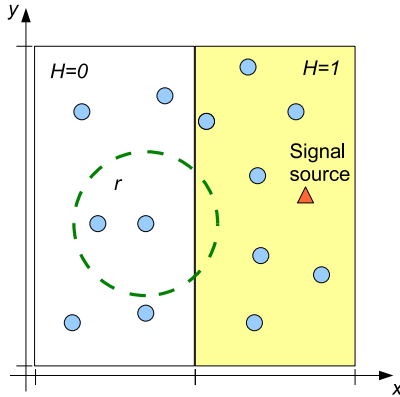
(b) Large-scale network: $K = 50$ randomly deployed nodes, with communication range r. Nodes in the left sector are under $\mathcal{H} = 0$, nodes in the right sector are under $\mathcal{H} = 1$.

Fig. 3. Simulation scenarios.

V. SIMULATION RESULTS

A. Simulation Scenarios

We evaluate the performance of the proposed algorithm in two different simulation scenarios: the small network of Fig. 3(a) and the large-scale, random network of Fig. 3(b).

The first case consists on $K = 6$ nodes; 3 of them experience the presence of a primary signal ($\mathcal{H} = 1$), while the other 3 nodes are located in a "spectrum hole" region ($\mathcal{H} = 0$). Each node can communicate with a limited number of neighbors, indicated by dotted lines in the figure. The second case is a large-scale network modeled as a "random geometric graph" [34], where $K = 50$ nodes are deployed randomly and can communicate with each other if their distance is less than r. It is assumed that nodes in the left part of the plane are under hypothesis $\mathcal{H} = 0$, while nodes on the right are in the presence of a signal. In all simulations, primary user signals are modeled as constant-envelope signals transmitted over a Rayleigh fading channel, such that the received signal amplitude changes at every sample. In some examples we assume the average SNR to be the equal for all nodes in the region with $\mathcal{H} = 1$, while in other examples we assume different average SNRs, due to different distances of sensor nodes from the signal source, or to other attenuation factors.

The performance of the proposed NP-BP algorithm is compared to that of the following alternative CED schemes:

- *CED-EGC-Cluster*, i.e., the test statistic (31) computed in a centralized way assuming ideal prior knowledge of clusters.

- *CED-EGC-Neighbors*, i.e., CED-EGC performed by each node using own and (1-hop) neighbors' data. This is equivalent to a conventional CED scheme, where each node acts as a local fusion center.

For a fair comparison, EGC is used for all CED methods. If knowledge of local SNRs is available, the OC coefficient $\frac{\rho_k}{1+\rho_k}$ can be inserted in CED and NP-BP test statistics (see Sec. IV-B), with no effect on the relative performance of NP-BP and CED approaches.

B. Results in the Small-Scale Scenario

Results for the small-scale scenario are reported in Figures 4, 5, and 6. The plot in Fig. 4(a) illustrates the false-alarm probability, computed for one of the nodes under $\mathcal{H} = 0$, namely node 4, and the detection probability, computed for one of the nodes under $\mathcal{H} = 1$, namely node 2, at three different time slots: $t = 1$, $t = 5$, and $t = 10$. For all slots, BP is stopped at the third iteration. Observe that at $t = 1$, the NP-BP algorithm reduces to single-user detection, because no observations are available, hence all variables $\Delta_{kj}^{(t)}$ are equal to 0. All three nodes under hypothesis $\mathcal{H} = 1$ are affected by Rayleigh fading and have in this case the same average SNR (-5 dB).. The plot shows that NP-BP significantly improves the performance of single-user energy detection (i.e., results at $t = 1$), in terms of both false-alarm and detection probabilities. The gap increases with time, as the system gradually learns the correlation parameters. At $t = 10$, NB-BP reaches exactly the ideal *CED-EGC-Cluster* performance, thus validating (37). On the contrary, the conventional *CED-EGC-Neighbors* method is suboptimal, mainly because the lack of an appropriate clustering procedure makes nodes fuse their information with neighbors that are under different conditions (e.g., node 4 with node 3). The other benefit of the NP-BP method over conventional CED, i.e., multi-hop collaboration, is less important in this small-scale example. Note that in this simulation the threshold is set like in the single-user case (7), therefore the achieved false-alarm probability is lower than the nominal rate α. The impact of the learning procedure is illustrated more clearly in Fig. 4(b), which shows the evolution of false-alarm and detection probability for all nodes in the network as a function of time. All nodes exhibit performance improvements thanks to the proposed learning strategy. The slope of the learning curves depends on the constant λ, as discussed in Sec. IV-A.

Variations of the previous simulation scenario are considered in Fig. 5. In Fig. 5(a) the threshold is reset using (34), with $|\mathcal{C}| = 1 + |\mathcal{N}_2| = 3$. In this case, the system achieves the nominal false-alarm rate α asymptotically[3] in t, while the detection probability is significantly improved and still consistent with the performance of *CED-EGC-Cluster* (with cooperative threshold as well). Fig. 5(b) shows the results obtained again in the small-scale network, but with different average SNRs for the three nodes under $\mathcal{H} = 1$. In this case the performance of the NP-BP method converges to the *CED-EGC-Cluster* curve (36) in the rightmost part of the plot, and it performs slightly better for $\alpha \to 0$. The reason is that

---

[3]In practice, for $t \approx 10$. Also note that expressions (7) and (34) are derived by applying the central limit theorem, and turn out to be slightly biased upwards for $\alpha \to 0$.
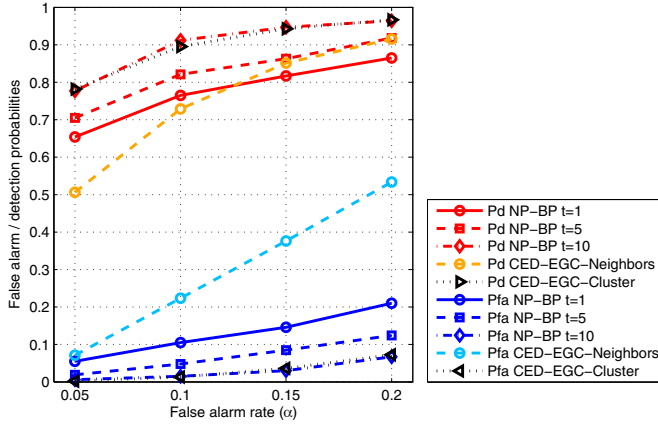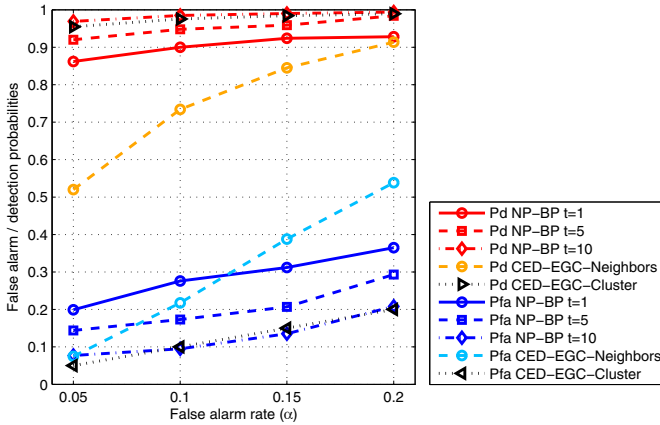
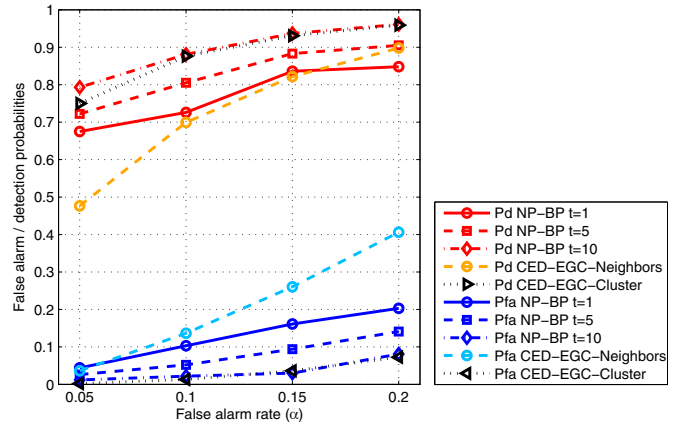(a) P_d for node 2, P_fa for node 4.
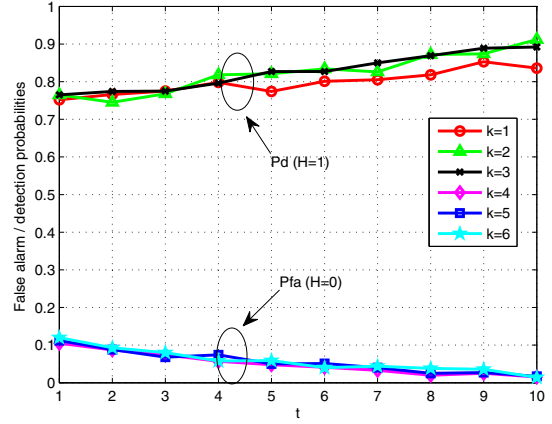
(b) Results for all nodes at $\alpha = 0.1$.

Fig. 4. Simulation results for the small-scale network of Fig. 3(a). Average SNR=$\{-5, -5, -5\}$ dB, Rayleigh fading. 3 iterations. (a) Single-node P_d and P_fa. (b) P_d, P_fa vs. t.

(a) Cooperative decision threshold (34).

(b) Different average SNR: $\{-4, -5, -7\}$ dB.

Fig. 5. Simulation results for the same scenario as in Fig. 4, but: (a) cooperative threshold $\eta_\mathcal{C}(\alpha)$ with $|\mathcal{C}| = 1 + |\mathcal{N}_2| = 3$; (b) different average SNR for nodes 1, 2, 3.

an additional advantage comes from the (negative) correlation with the nodes of the other cluster. Although this advantage is negligible in most cases, it becomes relevant when α is low and when the nodes in the cluster have different SNRs. To give insight into this fact, we compare in Fig. 6 the detection probability achieved (a) in the same scenario of the previous figure (two clusters, three nodes under $\mathcal{H} = 1$ and three under $\mathcal{H} = 0$), and (b) in the first cluster alone. It can be observed that in the second case the *CED-EGC-Cluster* curve is an upper bound, whereas in the presence of other nodes the bound can be attained and even passed. In all cases, however, the theoretical expression (36) provides useful information about the expected performance of the NP-BP method.

C. Results in the Large-Scale Scenario

We next consider the large-scale network of Fig. 3(b). The specific network configuration used in the simulation is depicted in Fig. 7(a). For nodes under $\mathcal{H} = 1$, the received signal is affected by Rayleigh fading and the average SNR varies from node to node, in a range between -8 and -1 dB. Results shown in Fig. 7(b) represent the false-alarm and detection probability averaged over all the nodes under

$\mathcal{H} = 0$ and $\mathcal{H} = 1$, respectively. Also in this scenario, NP-BP provides a substantial improvement compared to single-user detection as well as to *CED-EGC-Neighbors*. The gap here is lower than in the small-scale example, because results are averaged over all nodes, most of which are surrounded by neighbors under identical spectrum conditions. Thus, the main NP-BP gain is in this case multi-hop collaboration. The centralized *CED-EGC-Cluster* scheme is not considered here, as it would not be practical in a large-scale, multi-hop network. The threshold is set according to the single-user formula (7), hence the achieved false-alarm probability is lower than the nominal value.

D. Reweighted NP-BP

Finally we address the issue of convergence, and we compare the performance of standard BP with that of URW-BP. To this purpose, we consider again the small-scale network of Fig. 3(a), and we increase the number of iterations to 10 so as to appreciate the effect of loops. Results are reported in Fig. 8. In this scenario, standard BP does not provide satisfactory performance as loops degrade the quality of test statistics; as a consequence, the detection probability of BP is far from the
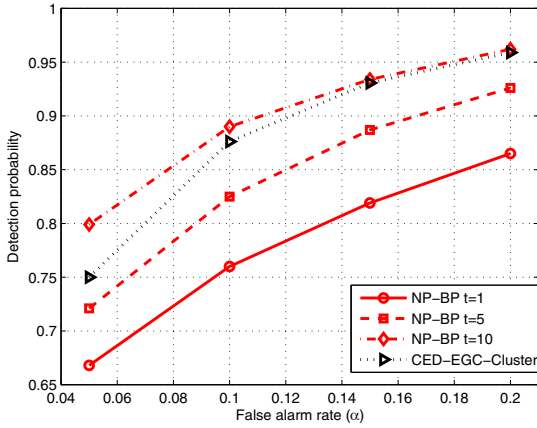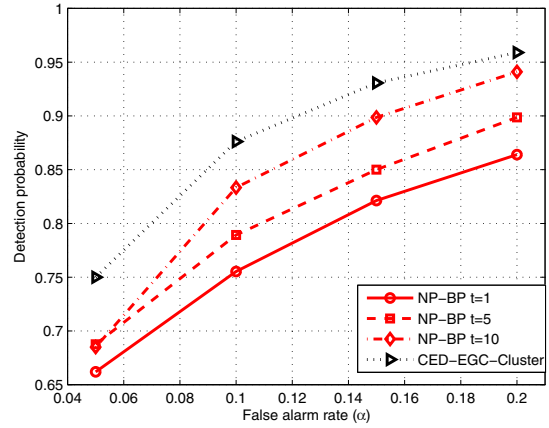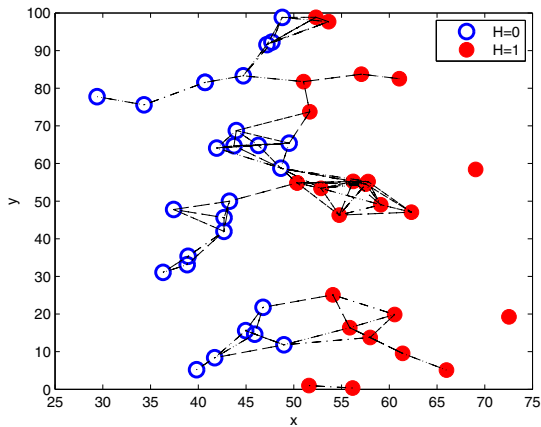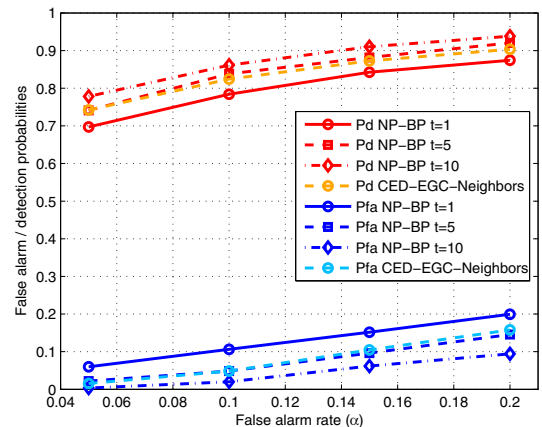
(a) $K = 6$.

(b) $K = 3$.

Fig. 6. Detection performance comparison: single cluster vs. two clusters. (a) Configuration of Fig. 3(a). (b) Only left cluster ($\mathcal{H} = 1$). Average SNR=$\{-4, -5, -7\}$ dB.

(a) Network configuration.

(b) Results.

Fig. 7. Simulation results for the large-scale network of Fig. 3(b). The average SNRs of nodes under $\mathcal{H} = 1$ are chosen from a uniform distribution in $[-8, -1]$ dB. Rayleigh fading. 3 iterations. The reported P_{d} and P_{fa} are averaged among all nodes under $\mathcal{H} = 1$ and $\mathcal{H} = 0$, respectively. In panel (a), edges represent links between neighboring nodes.

CED-EGC-Cluster curve. On the contrary, URW-BP restores the performance of NP-BP and slightly outperforms *CED-EGC-Cluster*. Therefore, whenever the number of iterations is comparable to the size of loops in the graph, the reweighted version of NP-BP (Sec. IV-E) can be used to counteract the effect of loops.

VI. CONCLUSIONS

In this paper we have proposed a novel approach for cooperative signal detection, called NP-BP, that combines the belief propagation algorithm with local Neyman-Pearson tests. This method is suitable for cooperative spectrum sensing in cognitive radio networks, as it provides a number of advantages compared to traditional approaches:

- Thanks to the NP formulation, it allows for a precise control of the false-alarm probability of each node.
- It operates in a fully decentralized manner, in contrast to other cooperative spectrum sensing schemes that require a central unit (fusion center) to process the data and make a final decision for the whole network.

- It achieves cooperation among nodes in a peer-to-peer fashion, thus ensuring robustness, flexibility, scalability.
- It performs automatic learning of correlations and clustering of the nodes in the network, hence it is suitable for heterogeneous as well as time-varying radio environments.

The performance of the proposed NP-BP algorithm has been evaluated analytically and by simulation results. It has been shown that, after a sufficient number of iterations and time slots, NP-BP provides nearly the same performance as cooperative energy detection applied separately by each cluster of the network – which would require *(i)* prior definition of clusters, *(ii)* selection of a fusion center for each cluster ("cluster-head"), and *(iii)* broadcast of the final decision from the cluster-head to all members of the clusters.

REFERENCES

[1] R. R. Tenney and N. R. Sandell Jr., "Detection with distributed sensors," *IEEE Trans. Aerosp. Electron. Syst.*, vol. AES-17, July 1981.
[2] R. Viswanathan and P. K. Varshney, "Distributed detection with multiple sensors: part I – fundamentals," *Proc. IEEE*, vol. 85, no. 1, Jan. 1997.
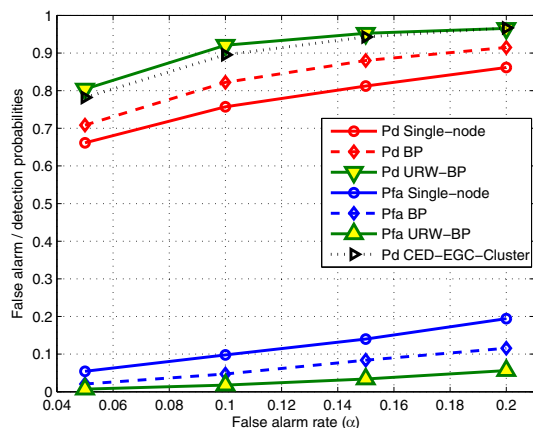
Fig. 8. Comparison between standard BP and URW-BP, in the same network of Fig. 3(a). Average SNR=$\{-5, -5, -5\}$ dB, Rayleigh fading. All results are for $t = 10$ time slots; 10 iterations per slot.

[3] R. S. Blum, S. A. Kassam, and H. V. Poor, "Distributed detection with multiple sensors: part II – advanced topics," *Proc. IEEE*, vol. 85, no. 1, Jan. 1997.

[4] D. Pados, P. Papantoni-Kazakos, D. Kazakos, and A. Koyiantis, "On-line threshold learning for Neyman-Pearson distributed detection," *IEEE Trans. Systems, Man, and Cybernetics*, vol. 24, no. 10, Oct. 1994.

[5] M. Xiang and J. Zhao, "On the performance of distributed Neyman-Pearson detection systems," *IEEE Trans. Systems, Man, and Cybernetics*, vol. 31, no. 1, Jan. 2001.

[6] D. Cabric, S. M. Mishra, and R. W. Brodersen, "Implementation issues in spectrum sensing for cognitive radios," *Proc. 2004 IEEE Asilomar Conference on Signals, Systems and Computers*.

[7] A. Ghasemi and E. Sousa, "Collaborative spectrum sensing for opportunistic access in fading environments," *Proc. 2005 IEEE Symposium on New Frontiers in Dynamic Spectrum Access Networks*.

[8] M. Gandetto and C. Regazzoni, "Spectrum sensing: a distributed approach for cognitive terminals," *IEEE J. Sel. Areas Commun.*, vol. 25, no. 3, Apr. 2007.

[9] A. Taherpour, M. Nasiri-Kenari, and S. Gazor, "Multiple antenna spectrum sensing in cognitive radios," *IEEE Trans. Wireless Commun.*, vol. 9, no. 2, Feb. 2010.

[10] S. Zarrin and T. J. Lim, "Cooperative spectrum sensing in cognitive radios with incomplete likelihood functions," *IEEE Trans. Signal Process.*, vol. 58, no. 6, June 2010.

[11] V. Saligrama, M. Alanyali, and O. Savas, "Distributed detection in sensor networks with packet losses and finite capacity links," *IEEE Trans. Signal Process.*, vol. 54, no. 11, Nov. 2006.

[12] A. Dogandzic and B. Zhang, "Distributed estimation and detection for sensor networks using hidden Markov random field models," *IEEE Trans. Signal Process.*, vol. 54, no. 8, Aug. 2006.

[13] E. B. Ermis and V. Saligrama, "Distributed detection in sensor networks with limited range multimodal sensors," *IEEE Trans. Signal Process.*, vol. 58, no. 2, Feb. 2010.

[14] H. Li, "Cooperative spectrum sensing via belief propagation in spectrum-heterogeneous cognitive radio systems," *Proc. 2010 IEEE Wireless Communications and Networking Conference*.

[15] F. Penna, R. Garello, and M. A. Spirito, "Distributed inference of channel occupation probabilities in cognitive networks via message passing," *Proc. 2010 IEEE Symposium on New Frontiers in Dynamic Spectrum Access Networks*.

[16] R. Tandra, S. M. Mishra, and A. Sahai, "What is a spectrum hole and what does it take to recognize one?" *Proc. IEEE*, vol. 97, no. 5, May 2009.

[17] Y.-C. Liang, Y. Zeng, E. C. Y. Peh, and A. T. Hoang, "Sensing-throughput tradeoff for cognitive radio networks," *IEEE Trans. Wireless Commun.*, vol. 7, no. 4, pp. 1326–1337, Apr. 2008.

[18] R. Tandra and A. Sahai, "SNR walls for signal detection," *IEEE J. Sel. Topics Signal Process.*, vol. 2, no. 1, Feb. 2008.

[19] Y. Zeng and Y.-C. Liang, "Spectrum-sensing algorithms for cognitive radio based on statistical covariances," *IEEE Trans. Veh. Technol.*, vol. 58, no. 4, May 2009.

[20] M. J. Wainwright and M. I. Jordan, "Graphical models, exponential families, and variational inference," *Foundations and Trends in Machine Learning* vol. 1, no. 1-2, Now Publishers, 2008.

[21] F. R. Kschischang, B. J. Frey, and H. A. Loeliger, "Factor graphs and the sum-product algorithm," *IEEE Trans. Inf. Theory*, vol. 47, no. 2, Feb. 2001.

[22] S. Zarrin and T. J. Lim, "Belief propagation on factor graphs for cooperative spectrum sensing in cognitive radio," *Proc. 2008 IEEE Symposium on New Frontiers in Dynamic Spectrum Access Networks*.

[23] H. Wymeersch, J. Lien, and M. Z. Win "Cooperative localization in wireless networks," *Proc. IEEE*, vol. 97, no. 2, Feb. 2009.

[24] M. Caceres, F. Penna, H. Wymeersch, and R. Garello, "Hybrid cooperative positioning based on distributed belief propagation," *IEEE J. Sel. Areas Commun.*, vol. 29, no. 10, Dec. 2011.

[25] Y. C. Liang, Y. H. Zeng, E. Peh, and A. T. Hoang, "Sensing-throughput tradeoff for cognitive radio networks," *IEEE Trans. Wireless Commun.*, vol. 7, no. 4, Apr. 2008.

[26] Z. Quan, S. Cui, and A. H. Sayed, "Optimal linear cooperation for spectrum sensing in cognitive radio networks," *IEEE J. Sel. Topics Signal Process.*, vol. 2, no. 1, Feb. 2008.

[27] J. Ma, G. Zhao, and Y. Li, "Soft combination and detection for cooperative spectrum sensing in cognitive radio networks," *IEEE Trans. Wireless Commun.*, vol. 7, no. 11, Nov. 2008.

[28] C. Sun, W. Zhang, and K. Ben, "Cluster-based cooperative spectrum sensing in cognitive radio systems," *Proc. 2007 IEEE ICC*.

[29] C. Guo, T. Peng, S. Xu, H. Wang, and W. Wang, "Cooperative spectrum sensing with cluster-based architecture in cognitive radio networks," *Proc. 2009 VTC2009 – Spring*.

[30] K. Murphy, Y. Weiss, and M. Jordan, "Loopy belief propagation for approximate inference: an empirical study," *Proc. 1999 Conf. on Uncertainty in Artificial Intelligence*.

[31] F. Penna, H. Wymeersch, and V. Savic, "Uniformly reweighted belief propagation for distributed Bayesian hypothesis testing," *Proc. 2011 IEEE Statistical Signal Processing Workshop*.

[32] H. Wymeersch, F. Penna, and V. Savic, "Uniformly reweighted belief propagation: a factor graph approach," *Proc. 2011 IEEE International Symposium on Information Theory*.

[33] R. Olfati-Saber and R. M. Murray, "Consensus problems in networks of agents with switching topology and time-delays," *IEEE Trans. Automatic Control*, vol. 49, no. 9, pp. 1520–1533, Sep. 2004.

[34] M. D. Penrose, *Random Geometric Graphs*. Oxford University Press, 2003.

Federico Penna (S '09) received the M.S. degree (2008, with Honors) and the Ph.D. degree (2012) in Communications Engineering from Politecnico di Torino, Italy. In 2008 he was a research engineer with Istituto Superiore Mario Boella, Torino, Italy. During his Ph.D. he spent three months as a visiting researcher at Chalmers University, Gothenburg (Sweden), and six months at UCLA, Los Angeles, CA (USA). He is currently a post-doctoral research fellow with the Fraunhofer Heinrich Hertz Institute in Berlin, Germany. His research interests include distributed signal processing, multi-sensor signal detection, and cooperative positioning.

Roberto Garello (SM '03) received the Dottorato di Ricerca in Ingegneria Elettronica, from Politecnico di Torino, Italy, in 1994. From 1994 to 1997, he was with the Radio Link Laboratory of Marconi Communications, Genova. From 1998 to 2001, he was an Associate Professor at the University of Ancona. Since November 2001, he has been an Associate Professor at Politecnico di Torino, where from 2006 to 2008, he served as Coordinator of the Communication Engineering degree. His main research interests are communication systems (xDSL, LTE, space links, indoor positioning), cognitive radio networks, and channel coding.